Journal of the Physical Society of Japan
Vol. 57, No. 7, July, 1988, pp. 2557-2564

Resonant Photoemission Study of Molybdenum Bronzes: $K_{0.3}MoO_3$, $K_{0.33}MoO_3$ and $K_{0.9}Mo_6O_{17}$

Kazuo TERASHIMA, Hideki MATSUOKA, Kazuo SODA,†
Shigemasa SUGA,† Ryoichi YAMAMOTO and Masao DOYAMA

Department of Materials Science and Metallurgy, Faculty of Engineering, The University of Tokyo, 7-3-1 Hongo, Bunkyo-ku, Tokyo 113
†Synchrotron Radiation Laboratory, Institute for Solid State Physics, The University of Tokyo, Tanashi-shi, Tokyo 188

(Received June 4, 1987)

The electronic structures of molybdenum bronzes $K_{0.3}MoO_3$, $K_{0.33}MoO_3$ and $K_{0.9}MoO_{17}$ have been systematically studied by means of the ultraviolet photoemission spectroscopy (UPS). Resonant photoemission spectra have been measured in the photon energy range from 32 eV to 100 eV. The measurements of total yield spectra have also been made on $K_{0.3}MoO_3$ and $K_{0.9}Mo_6O_{17}$. Resonant enhancements of the photoemission have been observed in the valence and conduction bands with the contribution from the Mo 4d states for the excitation around $h\nu=49$ or 50 eV. It is found that the resonant effect is very weak for the structures at a binding energy $E_B=4.6$ eV for $K_{0.3}MoO_3$ and $K_{0.33}MoO_3$. The magnitude of these resonances corresponds to the local electronic densities of Mo 4d states at the corresponding E_B and can be qualitatively explained by the simple band structure model.

§1. Introduction

Recently, molybdenum bronzes $A_xMo_yO_z$ (A:Li, Na, K, Rb, Cs and Tl) have received much attention because of their characteristic electrical properties related to low dimensionality and superconductivity.

Among potassium molybdenum bronzes, we have studied the electronic structures of the blue bronze $K_{0.3}MoO_3$, the red bronze $K_{0.33}MoO_3$ and the purple bronze $K_{0.9}Mo_6O_{17}$. The blue bronze $K_{0.3}MoO_3$ is a typical quasi-one-dimensional conductor[1,2] which exhibits a metal-to-semiconductor transition at $T_c=180$ K[3] with the formation of a charge density wave (CDW).[4] In the CDW phase below this transition temperature, the nonlinear electrical conduction[5] due to the dynamics of the CDW were observed. The crystal structure is monoclinic with 20 formula per unit cell.[6] Clusters of MoO_6 octahedra form an infinite sheet, separated by K ions. This layered material can be cleaved parallel to the b-axis as well as to the [102] direction. The red bronze $K_{0.33}MoO_3$ is well known as a semiconductor at all temperatures.[7] The crystal structure of the red bronze is also monoclinic with 12 formula per unit cell.[8] $K_{0.9}Mo_6O_{17}$ is a quasi-two-dimensional conductor which undergoes a transition due to the onset of a CDW below 120 K.[9] The crystal structure is trigonal and consists of four layers of MoO_6 octahedra perpendicular to the c-axis, separated by the layers of MoO_4 tetrahedra and KO_{10} icosahedra.[10] The cleavage plane is the (0001) plane.

In these materials, it is considered that the valence bands are hybridized σ and π bonding bands from the molybdenum 4d and oxygen s-p orbitals, and the conduction bands being π^* bands made up of a combination of molybdenum 4d t_{2g} orbitals and oxygen p orbitals. A potassium atom donates the 4s electron to the Mo 4d orbitals. Several photoemission studies have already been performed on this family of crystals in order to examine the energy band structures. Angle-resolved and angle-integrated ultraviolet photoemission spectroscopy (UPS) and X-ray photoemission spectroscopy (XPS) were performed for $K_{0.3}MoO_3$.[11-13] These angle-resolved UPS experiments were the first study for the mapping of the conduction bands structures of quasi-one-dimensional CDW systems. The UPS technique was also applied to $K_{0.9}Mo_6O_{17}$.[14]

In this study, we systematically examined the electronic structures of the blue bronze $K_{0.3}MoO_3$, the red bronze $K_{0.33}MoO_3$ and the purple bronze $K_{0.9}Mo_6O_{17}$ by means of ultraviolet photoemission spectroscopy using synchrotron radiation. Resonant photoemission study is employed to reveal the hybridization of molybdenum 4d orbitals with oxygen 2p orbitals in the valence and conduction bands. The measurements of total yield spectra have also been made on $K_{0.3}MoO_3$ and $K_{0.9}Mo_6O_{17}$. Some of the discussions in this paper has already been reported.[11,14]

§2. Experimental

Single crystals used in this study were grown by electrolytic reduction of a melt of K_2MoO_4 and MoO_3 as described before.[15,16] Samples were identified by the X-ray diffraction method and the electrical resistivity measurement. All the crystals are platelets of typical sizes of $1\times1\times0.5\ mm^3$ (for $K_{0.3}MoO_3$), $10\times10\times30\ mm^3$ (for $K_{0.33}MoO_3$) and $4\times4\times0.5\ mm^3$ (for $K_{0.9}Mo_6O_{17}$).

Photoemission measurements were performed on clean surfaces of samples cleaved in situ in ultrahigh vacuum (UHV) at more than 1×10^{-10} Torr at the second beam line of SOR-RING, the 0.4 GeV electron storage ring of Synchrotron Radiation Laboratory, Institute for Solid State Physics, the University of Tokyo. No noticeable oxidation was detected through the measurements. A combination of a Rowland-type monochromator and a double-stage cylindrical mirror analyzer was employed. The resolution of the monochromator was set to 0.2 eV at the photon energy ($h\nu$) of 50 eV and that of the analyzer to 0.2 eV. The angle-integrated photoemission spectra of $K_{0.3}MoO_3$, $K_{0.33}MoO_3$ and $K_{0.9}Mo_6O_{17}$ were measured at room temperature over the range of photon energy from 32 eV to 100 eV. Particular attention has been paid to the resonant behavior of Mo 4d emission near the Mo 4p→4d transition. The energy distribution curves (EDC) were normalized by the photon flux.

Total yield (TY) spectra for $K_{0.3}MoO_3$ and $K_{0.9}Mo_6O_{17}$ were also measured with the use of a pico-amperemeter over the photon energy range of $h\nu=32\sim100$ eV. The TY spectra are known to resemble absorption spectra in the core excitation region.

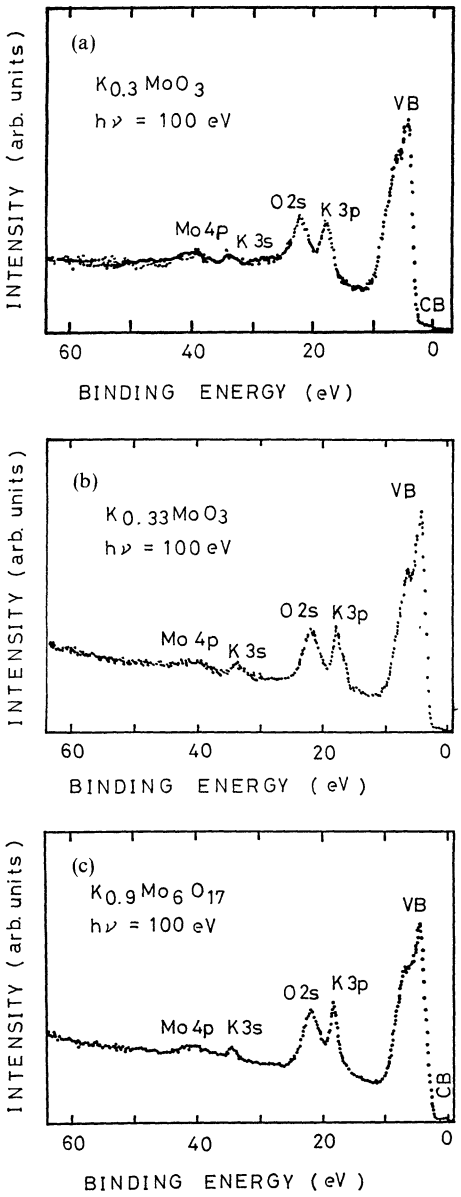

Fig. 1. The angle-integrated UPS spectra of (a) $K_{0.3}MoO_3$, (b) $K_{0.33}MoO_3$ and (c) $K_{0.9}Mo_6O_{17}$ for photon energy $h\nu=100$ eV measured at room temperature.

§3. Results and Discussion

In Figs. 1(a), 1(b) and 1(c), we present the typical overall angle-integrated UPS spectra of $K_{0.3}MoO_3$, $K_{0.33}MoO_3$ and $K_{0.9}Mo_6O_{17}$, respectively, measured for the photon energy

Table I. Core-level binding energies of $K_{0.3}MoO_3$, $K_{0.33}MoO_3$, $K_{0.9}Mo_6O_{17}$ and corresponding elements.

	$K_{0.3}MoO_3$	$K_{0.33}MoO_3$	$K_{0.9}Mo_6O_{17}$	elements (Cardona and Ley[17])
K 3p	18.1 eV	18.2 eV	18.5 eV	18.3 eV
O 2s	22.5 eV	22.4 eV	21.6 eV	—
K 3s	34.2 eV	34.3 eV	34.7 eV	34.8 eV
Mo 4p	40 eV	40 eV	41 eV	35.1 eV

($h\nu$) of 100 eV at room temperature. In all three curves, the structures with E_B (binding energy from the Fermi level) smaller than 10 eV are related to the valence and conduction bands, while those with E_B larger than 10 eV originate from individual inner core states, K 3p, O 2s, K 3s and Mo 4p. The binding energies of the inner core levels of these series determined from Figs. 1(a), 1(b) and 1(c) are listed in Table I with those of the corresponding elements. The structures of the valence and conduction bands of these three spectra are different, while those of the inner core states resemble each other. Figs. 2(a), 2(b) and 2(c) show the EDC of angle-integrated UPS spectra of the three materials for the photon energy $h\nu=60$ or 65 eV, where the mutual difference of the valence and conduction bands is clearly recognized between the three spectra.

Figures 3(a), 3(b) and 3(c) show a part of the result of the angle-integrated UPS spectra of $K_{0.3}MoO_3$, $K_{0.33}MoO_3$ and $K_{0.9}Mo_6O_{17}$, which were measured for different excitation photon energies between 32 and 100 eV. We have observed the remarkable increases in the photoemission intensities of most structures in all the three compounds around $h\nu=49$ or 50 eV. In order to obtain more detailed information of these resonant effects, we plotted the intensity of several peaks of the spectra for $K_{0.3}MoO_3$, $K_{0.33}MoO_3$ and $K_{0.9}Mo_6O_{17}$ as a function of the photon energy $h\nu$ in Figs. 4(a), 4(b) and 4(c), respectively. The intensities are evaluated from the peak height of the EDC spectra measured from the zero lines. Such curves are called the CIS (constant initial state) spectra. The CIS spectra correspond to the $h\nu$- dependence of the photoionization cross section for the same initial state. In Figs. 4(a), 4(b) and 4(c), it is noticed that the resonant effects for the structures at the binding energy $E_B=4.6$ eV in the valence bands are appreciably weak for $K_{0.9}Mo_6O_{17}$ and very weak for $K_{0.3}MoO_3$ and $K_{0.33}MoO_3$ in contrast to the resonance enhancement of other structures. The characteristic increases in photoemission intensities and the CIS spectra found around $h\nu=49$ or 50 eV can't be attributed to an overlap of Auger peaks, because we have ob-

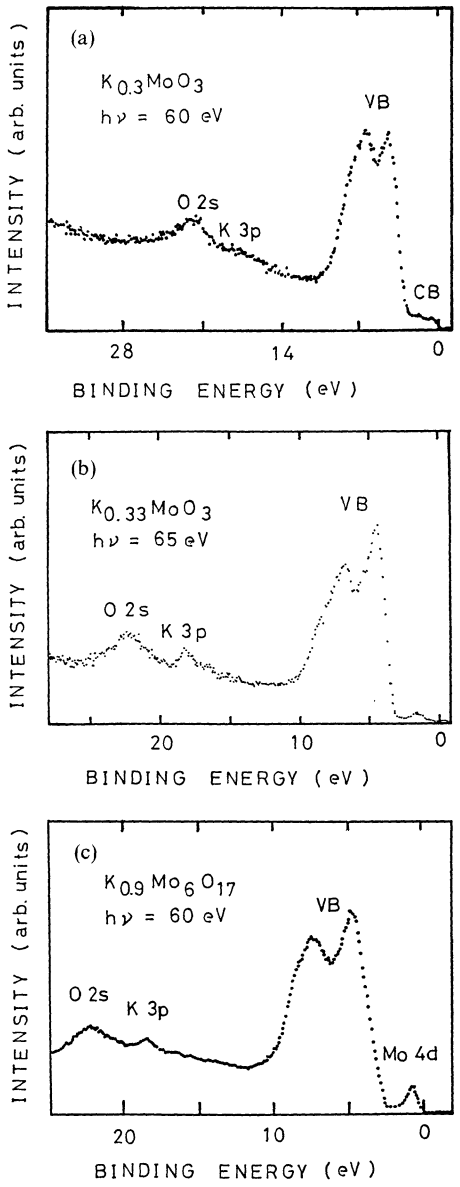

Fig. 2. The angle-integrated UPS spectra of (a) $K_{0.3}MoO_3$, (b) $K_{0.33}MoO_3$ and (c) $K_{0.9}Mo_6O_{17}$ for photon energy $h\nu=65$ or 60 eV measured at room temperature.

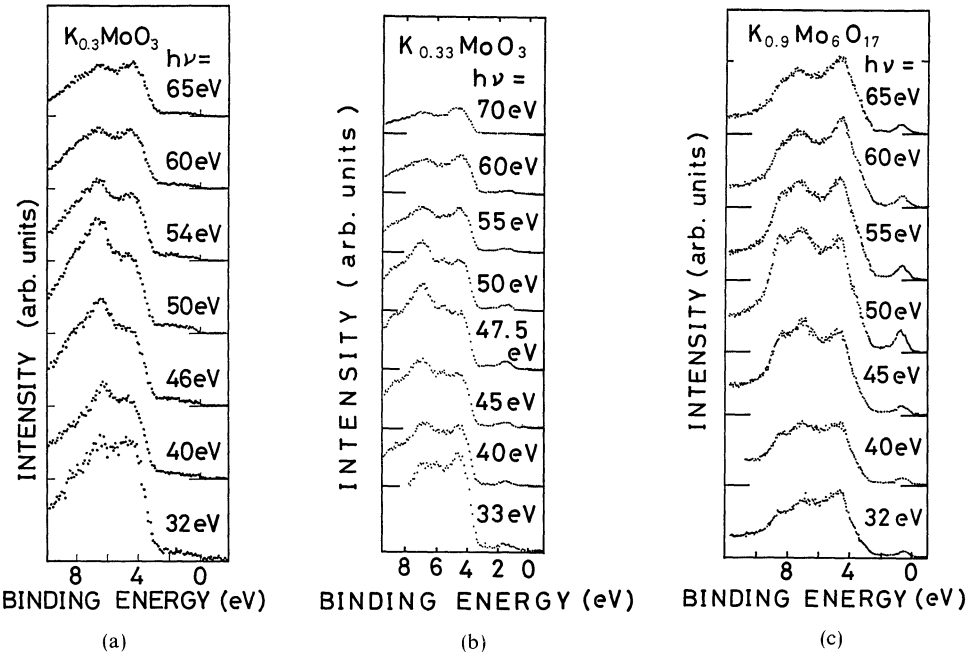

Fig. 3. Photon energy dependences of the angle-integrated UPS spectra for (a) $K_{0.3}MoO_3$, (b) $K_{0.33}MoO_3$ and (c) $K_{0.9}Mo_6O_{17}$ measured at room temperature.

served no peaks in the UPS spectra which move in parallel with the photon energy. The similar resonant enhancement effects were also detected in other Mo compounds such as $Cu_{1.8}Mo_6S_{7.6}$ with a completely different crystal structure.[18] Then we can confirm that this type of resonance is most likely ascribed to the $h\nu$-dependence of the atomic photoionization cross section of the Mo 4d states. Since the present spectra are measured by the angle-integrated mode, the band effects in the final state of the excitation from the 4d states may be smeared out. While the inner p core absorption is negligibly weak in the case of a nearly filled d shell metal,[19] the presence of a large amount of empty d states is playing the dominant role in both the absorption and the resonant photoemission process in molybdenum bronzes. Therefore, the resonant effects in these compounds can be qualitatively interpreted as resulting from an interference between the directly excited states of the Mo 4d valence or conduction electron and the final states realized through the Auger decay of the Mo 4p core excited states. For the resonant behavior of these three molybdenum bronzes, the following two processes are considered to occur:

$$\text{Mo } 4p^6 4d^n \longrightarrow 4p^6 4d^{n-1} + e \quad \text{(direct excitation)} \quad (1)$$

$$\text{Mo } 4p^6 4d^n \longrightarrow 4p^5 4d^{n+1} \quad (N_{2,3} \text{ excitation})$$
$$\longrightarrow 4p^6 4d^{n-1} + e \quad \text{(super Coster-Kronig decay)} \quad (2)$$

In the p inner core excitation, the excited electron far above E_F can be more properly described as the εd state.

The TY spectra of $K_{0.3}MoO_3$ and $K_{0.9}Mo_6O_{17}$ are shown in Figs. 5(a) and 5(b). These curves resemble the CIS spectra as shown in Figs. 4(a) and 4(c). The peak structures are also observed around $h\nu=49$ or 50 eV, respectively. As mentioned above, the TY spectrum is well known to resemble the absorption spectrum in the inner core excitation region. Thus, it is understood as the Mo 4p core excitation structure. Since the binding energy E_B of the Mo 4p core state measured by photoemission is about 40 or 41 eV, the peak of the CIS spectra and the absorption peak are delayed by about 9

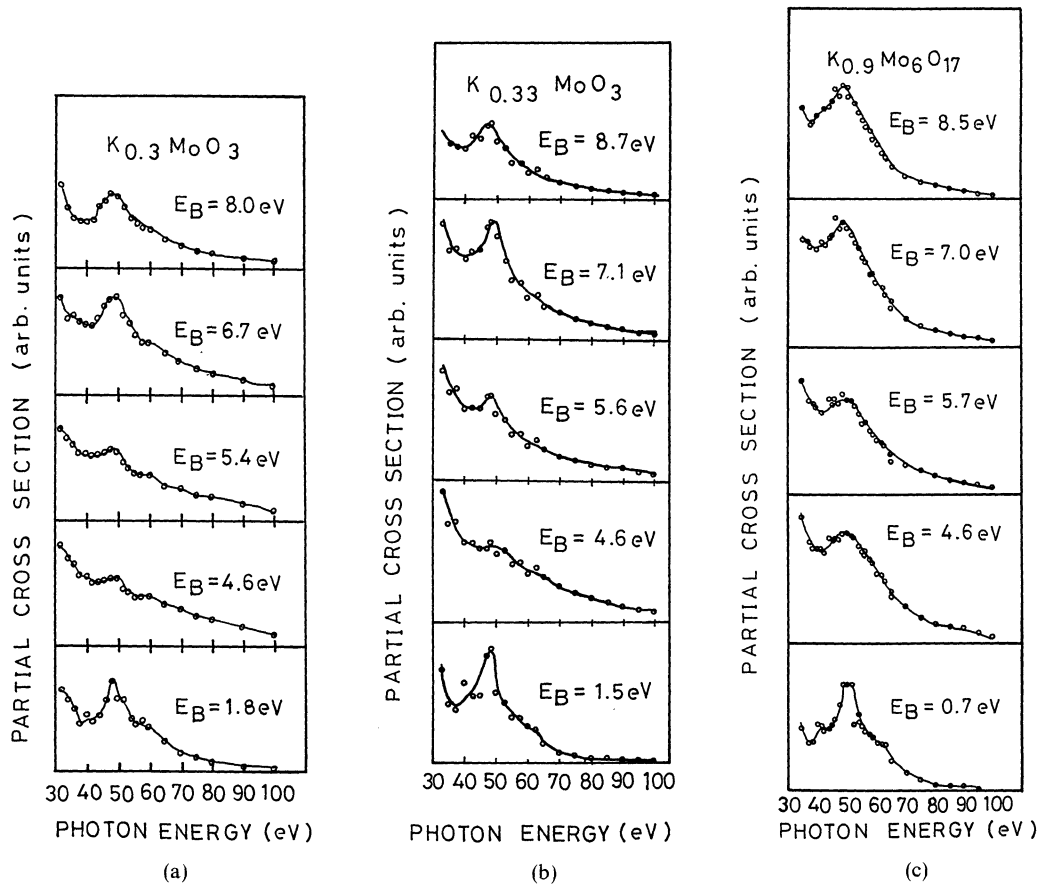

Fig. 4. Constant-initial-state (CIS) curves corresponding to several peaks of the spectra for (a) $K_{0.3}MoO_3$, (b) $K_{0.33}MoO_3$ and (c) $K_{0.9}Mo_6O_{17}$.

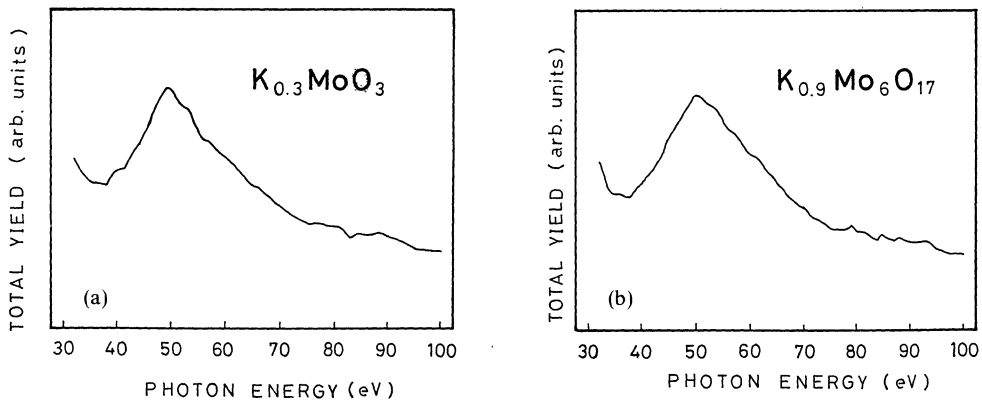

Fig. 5. Total yield spectra for (a) $K_{0.3}MoO_3$ and (b) $K_{0.9}Mo_6O_{17}$.

eV. Although there may exist a peak in the unoccupied density of states for the Mo 4d orbitals about 9 eV above the Fermi energy, such a large band width of Mo 4d states of more than 10 eV is rather unrealistic. The Coulomb and exchange interactions between the p core hole and d electrons as well as the centrifugal potential play essential roles in these delays.

Such delays were also detected not only in another Mo compound, $Cu_{1.8}Mo_6S_{7.6}$,[18] but also in other localized d electron systems, for examples, TiO_2.[20] In a qualitative sense, we can obtain the information of the local electronic density of Mo 4d states at the corresponding binding energy from the magnitude of the resonance in the CIS spectra. In order to relate the magnitude of the resonances around $h\nu=49$ or 50 eV to the electronic structures of these compounds, the simple band structure models of $K_{0.3}MoO_3$ and $K_{0.33}MoO_3$ are discussed at first. The band structures of $K_{0.9}Mo_6O_{17}$ can also be explained by the analogy with that of $K_{0.3}MoO_3$ and $K_{0.33}MoO_3$. The energy level schemes of $K_{0.3}MoO_3$ and $K_{0.33}MoO_3$ can be derived from the elementary MoO_6 octahedron as described previously.[2,21]

In a MoO_6 octahedron, the Mo 5s and 4d e_g orbitals combine with the three 2pσ orbitals of the oxygen (one per atom) to form a set of three bonding σ and three antibonding σ^* molecular orbitals. The Mo 4d t_{2g} orbitals combine with three oxygen per octahedron to give the bonding π and antibonding π^* bands. Three oxygen 2pπ orbitals per octahedron remain as nonbonding levels because they are of the wrong symmetry to combine with any of the Mo orbitals. Figure 6 represents the simple band structure model discussed above. The K atom donates the outer 4s electron to the 4d bands. Since the energy of the K 4s level is assumed to be high above the Fermi level, the energy level of unoccupied K^+ is not shown in Fig. 6. While σ and π bonding bands and pπ oxygen nonbonding levels form the fully filled valence bands, σ^* and π^* bands can form the conduction or the outermost valence bands. In these cases, σ^* bands are completely empty. As discussed above, the magnitude of the resonance corresponds to the local electronic density of Mo 4d orbitals at the corresponding binding energies. Therefore, if the rate of Mo 4d orbitals increases, the resonant enhancements in these CIS curves become stronger. From Figs. 4(a) and 4(b), it is clear that the resonant enhancements at $E_B=1.8$ (for $K_{0.3}MoO_3$) or 1.5 (for $K_{0.33}MoO_3$) eV in the conduction or the outermost valence bands are much larger than those at the other binding energies in the valence bands. On the

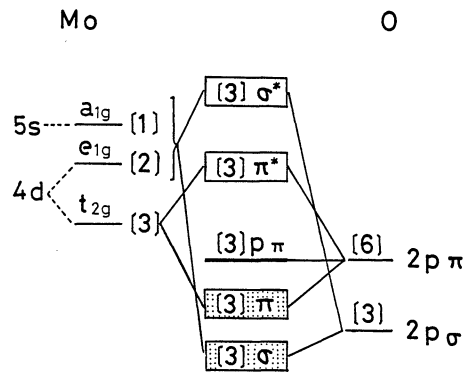

Fig. 6. Simple band structure model of $K_{0.3}MoO_3$ and $K_{0.33}MoO_3$ commencing with the elementary MoO_6 octahedron.

contrary, the resonant effects at $E_B=4.6$ eV corresponding to the shallower binding energy E_B region of the valence bands are very weak for both materials, whereas remarkable resonances are observed at the deeper binding energies in the valence bands. Moreover, the enhancements at the middle binding energies of the valence bands at $E_B=6.7$ (for $K_{0.3}MoO_3$) or 7.1 (for $K_{0.33}MoO_3$) eV seem to be larger than those at the deeper structures with $E_B=8.0$ (for $K_{0.3}MoO_3$) or 8.7 (for $K_{0.33}MoO_3$) eV. These points can be explained by this simple band structure model. As for the first point, the conduction (or the outermost valence) bands of these two compounds consist of π^* bands dominated by the Mo 4d orbitals, while the valence bands are made up of pπ, π and σ bands ascribed to the oxygen 2p orbitals or to those hybridized with Mo 4d orbitals. Therefore, it is reasonable that the resonant enhancements in the region of the conduction (or the outermost valence) bands are the largest at first. As for the second point, the very weak resonances at the shallow binding energies in the valence bands around $E_B=4.6$ eV are attributed to the existence of the nonbonding pπ valence bands. Finally, the degree of the hybridization of Mo 4d state of orbitals at the middle binding energy in the valence bands is larger than that of σ orbitals at the deeper binding energies as understood from Fig. 6. For this reason, the resonances at the middle binding energies in the valence bands at $E_B=6.7$ (for $K_{0.3}MoO_3$) or 7.1 eV (for $K_{0.33}MoO_3$) are larger than those at the deeper

binding energies in the valence bands at $E_B=8.0$ (for $K_{0.3}MoO_3$) or 8.7 eV (for $K_{0.33}MoO_3$). We can also explain the CIS spectra of $K_{0.9}M_6O_{17}$ by a simple model analogous to that of $K_{0.3}MoO_3$ and $K_{0.33}MoO_3$. In principle, the band structure of $K_{0.9}M_6O_{17}$ is similar to that of $K_{0.3}MoO_3$ and $K_{0.33}MoO_3$ originating from the elementary MoO_6 octahedron, while there are some differences derived from the existence of the layers of MoO_4 tetrahedra separating the four layers of MoO_6 octahedra. From Fig. 4(c), it is obvious that the resonant enhancements at $E_B=0.7$ eV in the conduction bands are much larger than those at the other binding energies in the valence bands. Besides, the enhancements at the middle binding energy region of the valence bands $E_B=7.0$ eV are larger than those at the deeper structures with $E_B=8.5$ eV. These two points are also observed in those of $K_{0.3}MoO_3$ and $K_{0.33}MoO_3$ and can be realized from the same energy level scheme as discussed above. On the other hand, the resonant effect at $E_B=4.6$ eV at the shallower binding energy E_B region of the valence bands is not so weak as the cases of $K_{0.3}MoO_3$ and $K_{0.33}MoO_3$. It suggests a contribution of the nonbonding orbitals of Mo 4d states originating from MoO_4 tetrahedron in the higher region of the valence bands near $E_B=4.6$ eV of $K_{0.9}Mo_6O_{17}$.

§5. Conclusion

The angle-integrated ultraviolet photoemission spectra of potassium molybdenum bronzes $K_{0.3}MoO_3$, $K_{0.33}MoO_3$ and $K_{0.9}Mo_6O_{17}$ have been systematically measured for the photon energies between 32 and 100 eV at room temperature. The measurements of total yield spectra have also been made on $K_{0.3}MoO_3$ and $K_{0.9}Mo_6O_{17}$. The CIS spectra in the region of the valence and conduction bands have shown the strong resonant enhancements around the photon energy $h\nu=49$ or 50 eV. While this energy is much greater than the binding energy of the Mo 4p core level measured by photoemission, these resonant effects are ascribed to the interference of the direct photoemission of Mo 4d states with the final state realized through the super Coster-Kronig decay of the Mo 4p core excited states leading to the same final state. A characteristic peak is also observed around $h\nu=49$ or 50 eV for total yield spectra, which is understood as the maximum of the Mo 4p→4d absorption. This energy is in coincidence with the energy of the resonant enhancement for the CIS spectra. Thus, the delay of the resonance from the core binding energy is attributed to the delay of the absorption peak.

The magnitude of these enhancements corresponds to the local electronic densities of Mo 4d orbitals at the corresponding binding energies. We can successfully explain the strength of these resonant effects by the simple band structure model.

Acknowledgment

The authors thank all members of the Synchrotron Radiation Laboratory of the Institute for Solid State Physics for their help with the UPS experiments. This work was supported in part by the Joint Research Project of the Institute for Solid State Physics, the University of Tokyo and a Grant-in-Aid of Scientific Research from the Ministry of Education, Science and Culture.

References

1) R. Brusetti, B. K. Chakraverty, J. Devenyi, J. Dumas, J. Marcus and C. Schlenker: *Recent Developments in Condensed Matter Physics*, ed. by J. T. Devreese, L. F. Lemmens, V. E. Van Doren and J. Van Royen (Plenum, New York, 1982) vol. 2, p. 181.
2) G. Travaglini, P. Wachter, J. Marcus and C. Schlenker: Solid State Commun. **37** (1981) 599.
3) W. Fogle and J. H. Perlstein: Phys. Rev. B **6** (1972) 1402.
4) J. P. Pouget, S. Kagoshima, J. Marcus and C. Schlenker: J. Phys. Lett. (Paris) **44** (1983) L11.
5) J. Dumas, C. Schlenker, J. Marcus and R. Buder: Phys. Rev. Lett. **50** (1983) 757.
6) J. Graham and A. D. Wadsley: Acta Crystallogr. **20** (1966) 93.
7) G. H. Bouchard, J. H. Perlstein and M. J. Sienko: Inorg. Chem. **6** (1967) 1682.
8) N. G. Stephanson and A. D. Wadsley: Acta Crystallogr. **18** (1965) 241.
9) R. Buder, J. Devenyi, J. Dumas, J. Marcus, J. Mercier, C. Schlenker and H. Vincent: J. Phys. Lett. (Paris) **43** (1982) L59.
10) H. Vincent, M. Ghedira, J. Marcus, J. Mercier and C. Schlenker: J. Solid St. Chem. **47** (1983) 113.
11) H. Matsuoka, K. Ohtake, R. Yamamoto, M. Doyama, H. Sakamoto, T. Mori, M. Fujisawa, K.

Soda and S. Suga: Physica **143B** (1986) 189.
12) J. Dumas, C. Schlenker, J. Y. Veuillen, R. Chevalier, J. Marcus, R. Cinti and E. Al. Khoury Nemeh: Synth. Met. **19** (1987) 937.
13) G. K. Wertheim, L. F. Schneemeyer and D. N. E. Buchanan: Phys. Rev. **B32** (1985) 3568.
14) K. Ohtake, H. Matsuoka, R. Yamamoto, M. Doyama, H. Sakamoto, T. Mori, K. Soda and S. Suga: J. Phys. C **36** (1987) 7207.
15) A. Wold, W. Kunnmann, R. J. Arnott and A. Ferretti: Inorg. Chem. **3** (1964) 545.
16) C. Escribe-Filippini, K. Konate, J. Marcus, C. Schlenker, R. Almairac, R. Ayroles and C. Roucau: Phil. Mag. B**50** (1984) 321.
17) M. Cardona and L. Ley: *Photoemission in Solid*, ed. by M. Cardona and L. Ley (Springer, Berlin, 1978) p. 264.
18) S. Suga, K. Soda, T. Mori, M. Yamamoto, K. Kitazawa and S. Tanaka: J. Phys. Soc. Jpn. **55** (1986) 2102.
19) P. O. Nilsson, C. G. Larsson and W. Eberhardt: Phys. Rev. **B24** (1981) 1739.
20) E. Bertel, R. Stockbauer and T. E. Madey: Phys. Rev. **B27** (1982) 1939.
21) P. G. Dickens and D. J. Neild: Trans. Faraday Soc. **64** (1968) 13.